A Framework for Stochastic Risk-Averse Decision Making in Hydrogen-Powered Intelligent Electric Vehicles Parking Management with Carbon and Green Certificate Considerations

Saber Kashiri[1], Jafar Siahbalaee[2*], Amangaldi Koochaki[3]

Abstract–Energy management in Intelligent Electric Parking Lots (IPL) plays a crucial role in achieving technical and environmental goals by utilizing renewable energy sources (RES) and hydrogen storage systems (HSS). This article proposes a framework for risk-averse decision-making in hydrogen-powered smart parking management, considering carbon considerations and green certifications. Given the uncertainty in input parameters such as solar radiation, temperature, wind speed, and IPL load, a probabilistic model is developed using a combination of two-point estimation method and Information Gap Decision Theory (IGDT). Furthermore, a combined optimization method, Differential Honey Badger Algorithm (DHBA), is employed to optimize operational costs, including energy procurement from the grid, electric vehicle (EV) charging costs in smart parking lots, and costs associated with green certifications and carbon emissions, as the main objectives of the optimization problem. The main idea of this article is for a typical IPL comprising a hydrogen storage system (HSS) consisting of a fuel cell, electrolyzer, and hydrogen storage tank, alongside load demand alongside RES. Additionally, alongside energy management, Demand Response (DR) management has also been optimized. Simulation results achieve all technical and economic objectives with the presence of renewable energy sources and electric vehicles, resulting in a 15.5% increase in profit. Furthermore, considering uncertainty leads to a 9.6% decrease in profit compared to the absence of these sources. Moreover, considering green certifications and carbon emissions results in a significant reduction in pollution emissions.

Keywords: Intelligent parking; Electric vehicles; Renewable energy sources; Honey Badger Algorithm optimization; Two-point estimation; Hydrogen storage system, Information Gap Decision Theory; Hydrogen storage; Carbon and green certificates.

1. Introduction

1.1. Motivation

In today's world, significant changes in energy consumption patterns and environmental attitudes have led to an increase in the use of renewable energy sources and the development of electric vehicles. The role of renewable energy sources in meeting a considerable portion of global energy demand indicates a deviation from fossil fuels [1,2]. This transition has been accompanied by the emergence of electric vehicles (EVs), driven by increasing awareness of the environmental challenges associated with conventional fuels. The depletion of fossil fuel reserves, coupled with intensified environmental pollution and increased energy consumption due to industrialization and population growth, underscores the need for sustainable alternatives such as electric vehicles [3,4]. The integration of EVs into power systems has witnessed significant growth in recent years. These vehicles, emblematic of technological advancements, pave the way for environmentally compatible transportation systems and provide an opportunity for countries to reduce dependence on fossil fuels and enhance grid reliability [5,6]. Additionally, they serve as the cornerstone of pursuing clean transportation solutions, aligning with the sustainability goals of modern cities. Simultaneously, policymakers are compelled to address the environmental consequences associated with EV charging and discharging [7].

Alongside these changes, new challenges emerge for the transportation and energy management industries.

1 Department of Electrical Engineering, Aliabad Katoul Branch, Islamic Azad University, Aliabad Katoul, Iran. Email:saberkashiri@aliabadiau.ac.ir

2* **Corresponding Author :**Department of Electrical Engineering, Aliabad Katoul Branch, Islamic Azad University, Aliabad Katoul, Iran Email:j.siahbalaee@aliabadiau.ac.ir

3 Department of Electrical Engineering, Aliabad Katoul Branch, Islamic Azad University, Aliabad Katoul, Iran. Email:koochaki@aliabadiau.ac.ir

Challenges include the need for improving existing technologies and conducting deeper research into optimizing Intelligent Parking Lot (IPL) management and energy storage in transportation systems [8,9]. Key aspects of these challenges include increasing energy efficiency, reducing environmental impacts, and devising appropriate strategies for integrating sustainable electric vehicles with the power grid. Decisive actions to address challenges arising from electric vehicle management in smart grids, including aspects such as grid integration, load management, and battery optimization, are necessary. Consequently, significant attention is directed towards optimizing EV charging/discharging processes and utilizing intermittent renewable energies, especially with the proliferation of smart parking lots (IPLs) driven by the increasing adoption of electric vehicles [6,10].

In addition to these challenges, the importance of carbon trading and green certifications in advancing environmental sustainability is recognized. Carbon trading mechanisms incentivize companies to reduce their carbon emissions by allowing them to buy and sell carbon credits. On the other hand, green certifications confirm the renewable source of electricity generated from renewable sources [11,12]. Integrating carbon trading considerations and green certifications into smart parking management is crucial for aligning environmental objectives with economic incentives. With these advancements, the concept of Intelligent Parking Lots (IPLs) emerges as a suitable solution for seamlessly integrating electric vehicles with renewable energy sources, energy storage systems, and carbon trading mechanisms. IPLs not only facilitate efficient energy management but also contribute to reducing carbon emissions and promoting the adoption of renewable energies [12].

To this end, optimizing smart parking management in comprehensive energy systems, with a focus on integrating electric vehicles, utilizing renewable energies, and combining carbon trading and green certification considerations, is important. This aims to address inevitable challenges in energy management, enhance the sustainability of transportation systems, and capitalize on economic incentives provided by carbon trading and green certifications. Continuous improvement and practical progress in this field guide technological innovations in energy and transportation, with positive impacts on the economic, environmental, and social dimensions of societies. Furthermore, optimal IPL management has the potential to inform policies and effective strategies in the energy and transportation sectors, providing innovative pathways to reduce reliance on fossil fuels, increase energy efficiency, and enhance environmental sustainability.

1.2. Related Works

In the field of energy management for charging/discharging electric vehicles (EVs) in parking lots, numerous studies have been conducted with a focus on various aspects and objectives. The literature review below provides an overview of research articles related to this topic along with their relevant sources.

• Electric Vehicles and Network Integration:

The continuous deterioration of the global environment and the depletion of fossil resources have turned energy conservation and reduction of greenhouse gas emissions in the transportation sector into a serious challenge. Today, due to environmental impacts and limited access to gasoline, there is a significant shift from fossil fuels to electric energy [13]. Therefore, electric vehicles (EVs) are introduced as suitable alternatives to fossil fuel vehicles [14]. These vehicles are not only energy consumers but also active components in the power system, which due to high uncertainty, pose various challenges for optimal system performance [15]. Electric vehicles (EVs) have advantages such as reducing energy consumption and greenhouse gas emissions, which are the main factors driving their widespread promotion [16]. G2V and V2G capabilities, along with the process of charging/discharging electric vehicles, provide potential benefits for electric vehicle owners and network operators through the charging/discharging of electric vehicles [17]. However, the unplanned entry of these vehicles into the smart distribution network undoubtedly will have negative effects such as increased load, losses, and more electrical fluctuations in the network [18]. However, hybrid and electric vehicles capable of connecting to the grid smooth the load curve during peak consumption hours and reduce vehicle owners' costs. Therefore, planning for the use of these vehicles in various usage scenarios is an undeniable reality [19], and for maximum utilization of these advantages, optimal electric vehicle parking performance must be thoroughly studied and managed [20]. These electric vehicles are influenced by various factors in the distribution network, such as different driving patterns and various charging schedules. This means that using smart control and management can create energy exchange between these vehicles and the power grid at specific times. Therefore, electric vehicles are a flexible type of load that can be considered as an example of demand response [18]. Furthermore, in article [21], a method of energy management involving electric vehicle (EV) load shifting to reduce energy costs has been discussed. Optimal charging and discharging management of electric vehicles in Intelligent Parking Lots (IPLs) in uncertain environments, as well as studies on optimal charging and discharging management of electric vehicles in IPLs in Tehran, have also been investigated in articles [22] and [23], respectively. Decisions regarding the charging and discharging of EV batteries for participation in storage and energy markets

have been specified [22]. An advanced model for smart parking with hydrogen storage systems, along with management of charging and discharging electric vehicles and transmission of renewable energies, has been examined in article [24]. Examination of a parking lot as a renewable energy-based microgrid with the aim of minimizing costs has been conducted in ref [7]. Planning based on certainty for optimal management of electric vehicle charging and discharging in IPLs under Demand Response Programs (DRP) and High Solar Scenarios (HSS) has been discussed in article [25].

• **Renewable Energy Systems and Smart Parking:**

Renewable energy systems can be used to address greenhouse gas issues in power systems [26], [27], and the penetration of renewable energy sources that produce clean energy can also control environmental issues [4,27]. These sources can be used to integrate with microgrids such as wind turbines, PV systems, microturbines, and fuel cell units. Additionally, smart parking facilities using a large number of EVs can be integrated with load management programs to enhance microgrid performance [30]. One interesting application of renewable energy sources is to provide power for electric vehicle charging stations [6]. Solar panels and wind turbines can be used in these stations.

• **Energy Management and Optimization:**

An advanced development model for smart parking with hydrogen storage systems, along with management of charging and discharging electric vehicles and transmission of renewable energies, has been examined in article [28]. Examination of a parking lot as a renewable energy-based microgrid with the aim of minimizing costs has been conducted in article [29]. Planning based on certainty for optimal management of EV charging and discharging in IPLs under Demand Response Programs (DRP) and High Solar Scenarios (HSS) has been discussed in ref [29].

• **Electric Vehicle Charging and Discharging Management:**

Decisions regarding the charging and discharging of EV batteries for participation in storage and energy markets have been specified [2]. An advanced model for smart parking with hydrogen storage systems, along with management of charging and discharging electric vehicles and transmission of renewable energies, has been examined in article [30]. Examination of a parking lot as a renewable

energy-based microgrid with the aim of minimizing costs has been conducted in ref [31] . Planning based on certainty for optimal management of electric vehicle charging and discharging in IPLs under Demand Response Programs (DRP) and High Solar Scenarios (HSS) has been discussed in the article [37].

1.3 Research Contribution

Contrary to previous research efforts, this study considers the preferences of electric vehicle (EV) owners and the operational constraints of the distribution system, along with uncertainties regarding carbon emissions and carbon certification. This pioneering approach offers a different perspective on energy management in Intelligent Parking Lots (IPLs) by integrating Renewable Energy Sources (RES) and Hydrogen Storage Systems (HSS) while addressing the needs and constraints of various stakeholders. Accordingly, this article introduces an innovative framework for decision-making in hydrogen-based smart parking management. It confirms the diverse preferences of electric vehicle owners and the complex operational constraints of the distribution system, providing a comprehensive solution that balances technical and environmental objectives.

To address inherent ambiguities in parameters such as solar radiation, temperature, wind speed, and IPL load, this study presents a probabilistic model that utilizes a combined approach of two-stage estimation and Information Gap Decision Theory. Additionally, optimization is employed using a Hybrid Belder Algorithm (DHBA) to reduce operational costs and pollution emissions. It also considers the costs of electric vehicle charging, financial implications of green certifications, and carbon emissions. The main objective of the article is to integrate a hydrogen storage system (HSS) into a conventional IPL configuration alongside demand response (DR) management to enhance operational efficiency and optimize sustainability. It emphasizes all technical and economic objectives, reflecting significant profitability and environmental benefits.

The primary research contributions are as follows:

• Integration of hydrogen storage and charge/discharge management in smart parking systems.

• Integration of wind and solar renewable energy sources in energy planning for smart parking.

• Optimization of charge/discharge decisions for electrolysis and fuel cell systems in hydrogen storage systems (HSS) to minimize operational costs and

green certification expenses.

- Evaluation of the role of electric vehicles as storage devices and their impact on load management and cost reduction.
- Implementation of a combined decision-making framework using Information Gap Decision Theory (IGDT) and a point estimation method to model uncertainty in system parameters.
- Utilization of the Hybrid Belder Algorithm (DHBA) for formulating the problem and achieving global optimal solutions.
- Consideration of carbon emissions and green certification for pollution reduction and increased penetration of renewable resources.
- Integration of demand response into planning and load management strategies.

1.4 Paper Organization

This article is generally divided into several important sections. The first section deals with the introduction and the explanation of the topic's significance. In the second section, an overview of the modeling and proposed framework is provided, including an explanation of the proposed model for smart parking, the use of renewable energy sources, and hydrogen storage, as well as the constraints and objectives of the modeling problem. The third section introduces the proposed algorithm for optimizing energy management. The fourth section is dedicated to the case study and the results obtained from the proposed models. In the fifth section, the results are discussed and compared with previous studies. Finally, the sixth section presents concluding remarks and research discussions.

2. Modeling and Problem Formulation

2.1 Main Title and Author affiliation

In the context of smart parking systems, where electricity exchange is involved, there is a need for a mechanism that prioritizes parking operation. This includes minimizing operating costs and potential penalties while maximizing revenue. To address this issue, the system's objective function is designed to maximize the profitability of Intelligent Parking Lots (IPL). Then, optimization models for IPL are developed to respond to various scenarios, aiming to minimize total costs while maximizing profits. The objective function is formulated as the sum of differences between incomes and expenses over all time

periods, including costs and revenues related to electricity buying and selling, load provisioning, energy transfer between parking lots and EVs, EV charging costs, fuel cells and hydrogen, load response costs, storage costs, and renewable energy production costs. Additionally, the cost of green certificates is also included[32].

$$Max(F)$$

$$= \sum_{t=1}^{T=24} \begin{bmatrix} \left(\left(P_{\text{sell-grid}}^t \times \pi_{\text{grid}}^t \right) - \left(P_{\text{buy-grid}}^t \times \pi_{\text{grid}}^t \right) \right) \times \Delta t \\ + \left(\pi_{\text{sell-load}}^t \times P_L^t \right) \times \Delta t \\ + \left(R_{PHEV-mG2V}^t + R_{PHEV-mV2G}^t \right) \times \Delta t \\ - \left(C_{FC}^t + C_{EL}^t + C_{\text{Tank}}^t \right) \times \Delta t \\ - \left(C_{\text{PHEV-mV2G}}^t + C_{\text{Cap}_{V2G}}^t + C_{\text{Penalty}}^t \right) \times \Delta t \\ - \left(C_{RES}^t \times \Delta t \right) \\ - \pi_{DR} \times \left(P_{DR}^t \right) \times \Delta t \end{bmatrix} \quad (1)$$

$$+ \sum_{t=1}^{T=24} \left[\pi_{grn} \times \left(P_{grn}^t - P_{re}^t \right) \right] \times \Delta t$$

Eq (1) outlines various components: $P_{\text{buy-grid}}^t$ and $P_{\text{sell-grid}}^t$ denote the purchased and sold power to the upstream network, while $\rho_{\text{sell-load}}^t$ signifies the energy selling price by IPL. $R_{PHEV-mV2G}^t$ represents revenue from V2G vehicle energy sales, $R_{PHEV-mG2V}^t$ from G2V vehicles, and $C_{\text{PHEV-mV2G}}^t$ for purchasing energy from V2G vehicles. The costs $C_{\text{Cap}_{V2G}}^t$ and C_{Penalty}^t stand for V2G vehicle capacity usage and charging non-compliance penalties, respectively. Additionally, C_{FC}^t, C_{EL}^t, and C_{Tank}^t indicate the operation and maintenance expenses for fuel cells, electrolyzers, and hydrogen tanks, while C_{RES}^t denotes the investment and operational costs of renewable energies.

2.2 Electric Vehicle Cost Modeling

The costs related to V2G electric vehicles consist of three parts, namely $C_{\text{Cap}_{V2G}}^t$, C_{Penalty}^t, and $C_{\text{PHEV-mV2G}}^t$. These costs are further explained below.

2.2.1 V2G Penalty Cost

Given the structure defined for smart parking, where the charging and discharging of electric vehicles are planned to ensure that the EV battery reaches the desired state of charge (SOC) by the time it leaves, if the actual final SOC falls short of the desired level, the operator is required to pay a penalty for failing to meet the charging requirements of V2G vehicles upon their exit from the smart parking. This penalty cost is calculated

using equation (2)[32].

$$C_{\text{Penalty}}^t = \sum_{v=1}^{my2C} \left(SOC_v^{\text{desired}} - SOC_v^{td}\right) \times \\ \times \rho_{\text{penalty}} \times \tau_v^d \qquad (2)$$

Where SOC_v^{desired} represents the desired final SOC of the vehicle, SOC_v^{td} is the actual final SOC of the vehicle, and ρ_{penalty} is the penalty fee tariff.

2.2.2. Cost of V2G Vehicle Capacity

Operators incur a cost per hour to encourage and motivate PHEV owners to participate in providing available capacity. This cost is outlined in equation (3)[32].

$$C_{\text{Cap-V2G}}^t = \sum_{v=1}^{my2G} \left(SOC_v^{\text{max}} - SOC_v^{\text{min}}\right) \times C^v \times \rho_{\text{cap.V2G}}^t \times \Lambda_v^t \qquad (3)$$

SOC_v^{max} and SOC_v^{min} represent the maximum and minimum SOC of the vehicle, respectively, C^v is the battery capacity, and $\rho_{\text{cap.V2G}}^t$ is the price of available capacity in period t. Λ_v^t is a binary variable indicating the vehicle's connection status in each period.

2.2.3. Cost of purchasing energy for V2G vehicles

To calculate the power exchange with the grid, the final and initial SOC levels are calculated, and based on that, the amount of exchanged power is determined. If $SOC_{t_v}^d$, the final SOC level, is less than $SOC_{t_v}^a$, the initial SOC level, the cost of purchasing energy from V2G vehicles is obtained from equation (4)[32].

$$C_{PHEV-mV2G}^l = \sum_{v=1}^{mv2G} \left(SOC_{t_v}^a - SOC_{t_v}^d\right) \times C^v \times \rho_{d,V2G}^t \times \tau_v^d \qquad (4)$$

where $\rho_{d,V2G}^t$ represents the price of discharging V2G vehicles in period t. C^v stands for battery capacity, and τ_v^d denotes a flag indicating the vehicle's movement time.

2.3. Modeling Electric Vehicle Profit

According to the profit objective function from selling energy to V2G and G2V vehicles using equations (5) and (6), the profit is calculated.

2.3.1. Profit from Selling Power to V2G

To compute the power sold to V2G, we need to establish the final and initial SOC of the vehicle, denoted as $SOC_{t_v^d}$ and $SOC_{t_v^a}$ respectively. By deducting the final SOC from the initial SOC, we can determine the amount of power charged into the V2G vehicle. The SOC at the time of departure, indicated as $SOC_{t_v^d}$, determines whether the EV is selling or purchasing energy. If the final SOC is lower than the initial SOC, the EV acts as a seller, while if it's higher, the EV acts as a buyer[32].

$$R_{PHEV-mV2G}^t = \sum_{v=1}^{mV_2G} \left(SOC_{t_v^d} - SOC_{t_v^a}\right) \times C^v \times \rho_{c\cdot V2G}^t \times \tau_v^d \qquad (5)$$

$\rho_{c\cdot V2G}^t$ represents the charging price for the V2G vehicle in a specific period, while mV2G denotes the collection of vehicles connected to the grid. τ_v^d serves as a flag indicating the vehicle's movement time.

2.3.2. Profit from selling power to G2V

Profit generated from selling power to G2V vehicles is calculated as a benefit for IPL, as they are regarded as loads, solely receiving power from the upstream network. This profit is computed using equation (6)[32].

$$R_{PHEV-m_{G2V}}^t = \sum_{v=1}^{m_{G2V}} \left(P_{v.c}^t \times \rho_c^t\right) \times \Lambda_v^t \times \Delta t \qquad (6)$$

In each period, $P_{v.c}^t$ represents the amount of power charged by G2V. ρ_c^t stands for the selling price of power, and Λ_v^t is a binary variable reflecting the vehicle's connection status.

2.4. Modeling Green Certificate Costs

Optimizing the performance of a smart parking system often involves integrating green certificates, which is effective in enhancing the production and use of renewable energy sources. Green certificates serve as evidence that energy production or consumption is derived from sustainable sources, thereby aiding in reducing greenhouse gas emissions. Including objective functions related to green certificates in system modeling plays a fundamental role in enhancing decision-making processes[11]. In the following section, the objective function for the tangible cost of green certificates for green certificates is specified as follows:

$$GreenCertificatesCost = \sum_{t=1}^{T} \left[\delta_{grn} \times \left(P_{grn}^t - P_{re}^t\right)\right] \qquad (7)$$

The objective function emphasizes the difference

between the amount of green energy produced (P_{grn}^t) and the amount of green energy consumed (P_{re}^t). This discrepancy indicates the potential for increasing green energy production or reducing green energy consumption from sustainable sources.

2.5. Modeling Renewable Resources

Renewable energy sources employed in this research consist of wind turbines and PV systems. The power generated by these units is simulated using equations (8) – (9), taking into account the uncertain characteristics of wind speed, solar radiation, and solar temperature[33].

$$P_{wind}^t = \begin{cases} 0 & V^t < V_c \ or \ V^t \geq V_c \\ \dfrac{V^t - V_c}{V_R - V_c} V_c \leq V^t < V_R \\ P_R V_R \leq V^t < V_F \end{cases} \tag{8}$$

$$P_{PV}(t) = \eta \times G(t) \times (1 - 0.005(T_a - 25)) \tag{9}$$

VC, VR, and VF represent the cutoff, grading, and unit shutdown wind speeds, respectively, while Vt denotes the predicted wind speed. Additionally, for PPV, the output power of the PV system, Lambda is the efficiency of the PV array, G(t) is the hourly solar radiation, and Ta is the hourly ambient temperature.

The cost associated with using renewable resources includes both investment and operational costs of renewable resources[32].

$$C_{RES}(t) = \sum_g c_g^{RES} + \sum_g c_g^{edg} P_u^{RES} \tag{10}$$

Here, c_g^{RES} stands for the capital investment cost, c_g^{edg} refers to the operational cost of renewable resources, and P_u^{RES} represents the power obtained from photovoltaic and wind turbine sources.

2.6. Hydrogen Storage Modeling

In this study, the hydrogen storage system (HSS) comprises three main parts: hydrogen storage tanks (HST), fuel cells (FC), and electrolyzers. The proposed HSS will be used as a sub-process during both peak and off-peak consumption periods. During off-peak hours when electricity prices are low due to minimal energy transactions, the electrolyzer transforms electrical power into hydrogen, which is then stored in HSTs. Conversely, during peak consumption periods when electricity pricesrise, FCs convert the stored hydrogen in HSTs back into electrical power. The hydrogen produced by electrolysis is compressed and stored in a pressure vessel[32].

2.6.1. Electrolyzer Modeling

Modeling the electrolyzer involves its use in separating water into H2 and O2 elements by supplying a direct current to its electrodes. The electrolysis output power in each cycle t, $P_{EL-Tank}^t$ can be calculated using Equation (11) [11,32].

$$P_{EL-Tank}^t = P_{IPL-EL}^t \times \eta_{EL} \tag{11}$$

where P_{IPL-EL}^t is the electrical power delivered from IPL to the electrolyzer and η_{EL} is the efficiency of the electrolyzer.

2.6.2. Electrolyzer Modeling

The electrolyzer is employed to split water into H2 and O2 components by delivering a direct current to its electrodes. The power output of electrolysis in each cycle t can be computed using equation (11) [11,32].

$$P_{\text{Tank-FC}}^t = \frac{P_{FC-tPL}^t}{\eta_{FC}} \tag{12}$$

where P_{FC-tPL}^t denotes the power transmitted from the fuel cell to IPL, and η_{FC} represents the fuel cell efficiency.

2.6.3. Hydrogen Tank Storage Modeling

The hydrogen generated through electrolysis undergoes compression and is subsequently stored in a pressurized tank. The quantities of hydrogen stored in the tank and discharged from it to the fuel cell are computed using equations (13) and (14) respectively[11,32].

$$H_{EL-\text{Tank}}^t = \frac{P_{EL-\text{Tank}}^t}{E_{H_2}} \tag{13}$$

$$H_{\text{Tank}-FC}^t = \frac{P_{\text{Tank}-FC}^t}{E_{H_2}} \tag{14}$$

where E_{H_2} represents the energy of hydrogen per kilogram (kWh/kg).

The energy condition of the stored hydrogen in the tank is described using a dynamic pressure model presented in equation (15). Taking into account the initial state, its amount can be calculated hourly based on the system's performance, either by charging or discharging hydrogen. The energy stored in the tank for each interval can be determined using equation (15).

$$M_{\text{Tank}}^t = M_{\text{Tank}}^{t-\Delta t} + (H_{EL\text{-Tank}}^t - H_{\text{Tank}-FC}^t \times \eta_{\text{Tank}}) \times \Delta t \tag{15}$$

M_{Tank}^t and $M_{\text{Tank}}^{t-\Delta t}$ indicate the amount of stored hydrogen in the tank in periods t and t-Δt, respectively. Moreover, Δt represents the duration of each period, which is one hour, and represents the efficiency of the tank.

2.7. Electric Vehicle Modeling

In this research, owners of PHEVs are encouraged to engage in the V2G program through various incentives provided by the IPL manager. Vehicles participating in this program are termed V2G, while those not participating are labeled G2V. Energy management can be carried out by restricting battery charging or discharging based on factors such as entry time, the presence of electric vehicles in the parking lot, and the forecasted hourly price. During periods when PHEVs are linked to the IPL, the SOC of each PHEV (SOC_v^t) is influenced by the SOC of the electric vehicle in the previous period ($SOC_v^{t-\Delta t}$) and its current charging or discharging status, as per equation (16). This equation considers parameters such as battery capacity and the times of vehicle entry and exit to determine battery charging and discharging power as well as their efficiencies[26,28].

$$SOC_v^t = SOC_v^{t-\Delta t} + \left(\frac{\eta_c^v P_{v.c}^t}{C^v} - \frac{P_{v.d}^t}{\eta_d^v C^v}\right) \times \Delta t; t_v^a < t \le t_v^d \quad (16)$$

$P_{v.c}^t$ and $P_{v.d}^t$ stand for the charging and discharging power of the battery, respectively. Moreover, η_c^v and η_d^v represent the efficiency of charging and discharging, while t_v^a and t_v^d denote the battery capacity and entry and exit times, respectively.

2.8. Modeling Demand Response

In the realm of optimal IPL management, harnessing the flexibility of demand-side response is crucial for optimizing energy consumption and ensuring efficient operation. This study introduces an integrated DR model, where IPL load is transformed into a DR source, enabling dynamic pairing and conversion of multiple energy sources. The mathematical representation of this integrated DR model is as follows[34]:

$$P_{DR}^t = [Load_{base}^t - Load_{DR}^t].\Delta t; \forall t \in T \quad (17)$$

$$Load_{DR}^t = [DR_t \times Load_{base}^t].\Delta t; \forall t \in T \quad (18)$$

$$0 \le DR_t \le 1; \forall t \in T \quad (19)$$

2.9. Constraints Modeling

Considering the objective function outlined in section 2.1 for resolving this optimization problem, various equality and inequality constraints are involved. Thus, it is assumed that IPL is linked to an upstream network in a

chain, and the objective functions are fine-tuned while adhering to the described limitations [26,28,32].

$$P_{IPL-EL}^t + P_L^t + P_c^t + P_{\text{sell-grid}}^t$$
$$= P_{wind}^t + P_{pv}^t + P_{FC-IPL}^t$$
$$+ P_{buy-grdd}^t + P_d^t$$
$$\quad (20)$$

$$P_{EL}^t \times \eta_{El} = D^t{}_2 + P_{FC}^t + H_{\text{EL-Tank}}^t$$
$$- H_{\text{Tank}-FC}^t \quad (21)$$

$$P_{\text{grid}}^t ; \left| P_{\text{gnid}}^t \right| \le P_{\text{grid}_{max}} \quad (22)$$

$$SOC_v^{min_v^{t_{max}}} \quad (23)$$

$$-P_{v,d}^{max_{v,c}^{t_{max}}} \quad (24)$$

$$SOC_v^{t_d} < SOC_v^{desired} \quad (25)$$

$$-P_{EL}^{max_{HFC}^{t_{max}}} \quad (26)$$

$$M_{\text{Tank}}^t \le M_{max} \quad (27)$$

$$M_{\text{Tank}}^0 = M_{\text{Tank}}^{24} \quad (28)$$

$$P_{wt}^{min_{wt}^{t_{max}}} \quad (29)$$

$$P_{pv}^{min_{pv}^{t_{max}}} \quad (30)$$

The constraints can be summarized as follows:
Equation (20) ensures a power balance within IPL, accounting for the total charging and discharging power of all PHEVs in the given period. Equation (21) maintains a balance in hydrogen production. Equation (22) limits the maximum capacity of the transmission line connected to the upstream network. Constraint (23) ensures that the energy charged into and discharged from the battery remains below its capacity and energy content, respectively. Constraints (24) and (25) set limits on the maximum charging and discharging power, respectively. Constraint (26) guarantees that the final output capacity does not exceed the desired final capacity. Constraints (27) and (28) establish limits on the maximum electrolysis and fuel cell power, as well as the maximum capacity of the hydrogen tank. Equation (28) maintains that the mass of hydrogen in the tank by the end of the operating period equals that at the start of the study day, ensuring sufficient hydrogen availability for the next day's operation. Constraints (29) and (30) define the maximum and minimum power generation capacities of

wind and solar renewable sources.

3. Optimization Method

In this section, an optimization method is introduced to solve the optimization problem of managing the IPL. The TPEM algorithm is also described.

3.1. Honey Badger Algorithm (HBA):

3.1.1. Inspiration

The Honey Badger Algorithm (HBA) is a metaheuristic algorithm proposed by Hashem et al. in 2022[35]. The algorithm imitates the foraging behavior of honey Badger. To find a food source, a honey bee either smells or follows the dance of a guide bee. The first mode is called the "scouting mode," and the second mode is called the "exploitative mode." In the scouting mode, the bee uses its sensing ability to approximate the location of the food source. When it reaches the area, it moves around to choose a suitable spot for collecting the food. In the exploitative mode, the bee follows the dance of a guide bee to find and exploit the food directly.

3.1.2. Proposed Mathematical Model:

As discussed earlier, the HBA algorithm is divided into two phases: the "scouting phase" and the "exploitative phase." In this section, the mathematical formulation of the HBA algorithm is explained. The HBA algorithm is equipped with both exploration and exploitation phases, making it a global optimization algorithm. The stages of the HBA algorithm are as follows:

Step 1: Initialization

The initial population size and their corresponding positions of honey Badger are determined based on the initial equation:

$$x_i = lb_i + r_1 \times (ub_i - lb_i) \tag{31}$$

r1 is a random value between 0 and 1. In this algorithm, xi represents the position of the honey badger that points to a candidate solution in a population of N individuals, while lb and ub are the lower and upper bounds of the search domain, respectively.

Step Two: Intensity Definition

Intensity refers to the concentration of the scent of the prey and the distance between it and the honey badger. Ii represents the intensity of the prey's scent. If the scent is strong, the movement will be fast, and vice versa, according to the inverse square law and the following equation.

$$I_i = r_2 \times S/4\pi d_i^2$$
$$S = (x_i - x_{i+1})^2 \tag{32}$$
$$d_i = x_{prey} - x_i$$

where S represents the strength of the source or the concentration power (prey location), and di indicates the distance between the prey and the i-th honey badger.

Step Three: Updating the Density Factor

The density factor (α) randomizes the variable over time to ensure a smooth transition from exploration to exploitation. The updating of the diminishing coefficient α, which decreases with iterations to reduce randomness over time, is governed by the following equation[35].

$$\alpha = C \times exp(-it/it_{max}) \tag{33}$$

Step Four: Escaping Local Optima

This step, along with the two following steps, is used to escape from local optima. In this regard, the proposed algorithm utilizes a flag F to change the search direction, allowing agents to explore high-opportunity areas for accurate scanning of the search space.

Step Five: Updating Representative Positions

As mentioned before, the updating process of the HBA positions (xnew) is divided into two phases: "excavation phase" and "honey phase."

• Excavation Phase

During the excavation phase, a honey badger performs a cardio vectored movement, as shown in Fig. 1. The cardio vectored movement can be simulated with the following equation:

$$x_{new} = x_{prey} + F \times \beta \times I \times x_{prey}$$
$$+F \times r_3 \times \alpha \times d_i \times |cos(2\pi r_4)|$$
$$\times [1 - cos(2\pi r_5)] \tag{34}$$

where β is the position of the prey, which represents the best global position found so far. In other words, it is the global best position. β (default value 6) indicates the honey badger's ability to sense the prey. di is the distance between the prey and a honey badger. r3, r4, and r5 are three different random numbers between 0 and 1. F acts as a flag that changes the search direction, determined using the following equation:

$$F = \begin{cases} 1 & if \, r_6 \leq 0.5 \\ -1 & else \end{cases} \tag{35}$$

In the excavation phase, a honey badger strongly relies on

the intensity of the smell of prey (I) represented by Xprey, the distance between the honey badger and the prey (di), and the search factor variable with time (α). Additionally, during the excavation activity, a honey badger may encounter any hindrance that allows it to find an even better hunting location (see Fig.1).
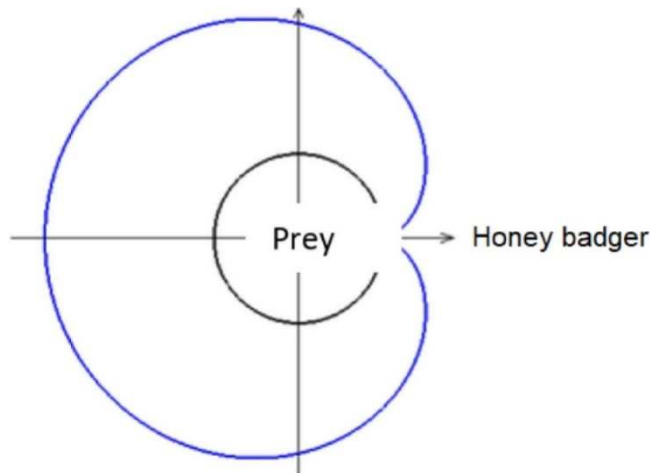
Fig. 1. Excavation Phase: The blue pattern represents the intensity of the smell (I), and the black circular line indicates the location of the prey[35].

- Honey Phase

When a honey badger follows the guidance of a bird in the honey phase to reach the beehive, its movement can be simulated using a similar equation.

$$x_{new} = x_{prey} + F \times r_7 \times \alpha \times d_i \tag{36}$$

In this equation, xnew refers to the new position of the honey badger, while xprey represents the location of the prey. The values of F and α are determined using the provided equation. From this equation, it can be observed that a honey badger, based on distance information, searches near the location of the prey (xprey) that has been found so far. In this phase, the search is influenced by the search behavior, which varies with time (α). Additionally, a honey badger may encounter the flag F, indicating potential disruptions during the search process.

3.3. Differential Honey Badger Algorithm (DHBA):

The HBA algorithm, due to its utilization of evolutionary strategies and effective social learning, maintains a balanced exploration of both local and global search spaces. Consequently, it exhibits considerable power and performs better in solving problems with real-valued functions. Furthermore, the division of the population into multiple groups has enabled the HBA algorithm to conduct rapid searches with suitable convergence characteristics. Essentially, the population division into groups or societies encourages individuals to explore different directions,

significantly increasing the diversity of mutations among them. Each member of the best community covers a specific region of the problem space. In comparison to its excellent capability, the HBA algorithm is relatively simple, requiring only one control parameter besides the population. This optimal control parameter value has been calculated in this study, eliminating the need for additional computations by the user. Additionally, to enhance its efficiency and convergence, a new phase has been added to this algorithm in this paper. In this new phase, the Differential Evolution (DE) [36] algorithm operator has been employed as the fifth phase of the algorithm, added through the following relationship.

$$N \quad (i) = \begin{cases} N \quad (i) \, rand(0,1) < CR \\ Nt(i) \, ot \quad erwise \end{cases} \tag{37}$$

4. Modeling uncertainty

Modeling uncertainty is a critical aspect of decision-making processes, especially when dealing with complex systems or situations where outcomes are not entirely predictable. Two common approaches to managing uncertainty are interval estimation and decision theory. Interval estimation involves assessing the best and worst-case scenarios to provide a wide spectrum of possible outcomes. On the other hand, decision theory focuses on identifying the maximum level of uncertainty that a decision-maker can tolerate, particularly when significant uncertainty exists. The rationale for combining these two methods lies in their complementary nature. In many real-world scenarios, the data used in decision-making predictions are often forecasted, and their performance is assumed to be symmetric. However, this assumption may not always hold true, especially when dealing with highly uncertain situations. By integrating interval estimation with decision theory, we can employ a structured approach to decision-making while also encompassing the range of probabilities provided by interval estimation. This combination allows decision-makers to consider not only the predicted data but also potential deviations from these predictions. Essentially, using interval estimation for probabilistic data enables a more comprehensive assessment of uncertainty and enhances the robustness of the decision-making process.

4.1. Two-Point Estimation Method (TPEM):

The two-point estimation method (TPEM) is well recognized as a prominent approximation technique owing to its exceptional precision and efficient computational speed [37]. Consequently, this research utilizes a TPEM-based approach to mitigate uncertainties associated with wind, solar, and load factors. The disparity between observed and projected values indicates the level of uncertainty. The use of less accurate methodologies for

managing uncertainty leads to a significant reduction in implementation costs. Various modeling methodologies are used depending on the nature of the issue and the presence of unknown variables. System operators may use TPEM to effectively manage uncertainties due to its high accuracy and efficient processing time[37]. The TPEM-Hong technique is a valuable strategy for addressing unclear matters, including random factors and statistical data. A comprehensive understanding of the probability density distributions of the parameters is not necessary[38]. The operational methodology of this strategy is grounded on the use of the moment-based approach to effectively manage unpredictable input parameters.

The process of calculating the moments of the output variables for the mid-term energy planning

problem can be summarized in the following steps[38]:

1- First, determine the number of random input variables, denoted by m.

2- Set the vector of the j-th output variable moments to zero: E(Yj) = 0.

3- Set t = 1 (t = 1, 2, ..., m).

4- Determine the two standard locations:

$$xi = \mu + \sqrt{2}.\sigma.erf^{-1}(2r-1) \quad (38)$$

$$\xi_{t,i} = \frac{\lambda_{t,3}}{2} + (-1)^{3-i}.\sqrt{\lambda_{t,4} - \frac{3}{4}\lambda_{t,3}^2} i = 1,2 \quad (39)$$

where λt, 3 are the skewness and λt, 4 are the kurtosis of the input random variable xt.

5- Determining two locations xt,i:

$$x_{t,i} = \mu_{t,i} + \xi_{t,i}\sigma_{t,i} i = 1,2 \quad (40)$$

where μxt and σxt are the mean and standard deviation of xt, respectively.

6- Implementation of IPL energy planning and management algorithm for both locations xt,i using two variable input vectors:

$$x_i = [\mu_{x1}, \mu_{x2}, \ldots, x_{t,i}, \ldots, \mu_{xm}]i = 1,2 \quad (41)$$

where μxk (k = 1, 2, …, m; and k ≠ t) are the average values of the remaining random input variables.

7- Determination of weight coefficients:

$$w_{t,i} = \frac{(-1)^{3-i}}{\xi_{t,i}(\xi_{t,1}-\xi_{t,2})} i = 1,2 \quad (42)$$

8- Update E(Yj):

$$E(Y^j)$$
$$= E(Y^j) + \sum_{i=1}^{2} w_{t,i}[F(X^j)] \quad (43)$$

9- Repeat steps 4 to 8 for t = t + 1 until the list of random input variables is finished.

10- Implementation of the medium-term planning algorithm of the distribution network using the input variable vector:

$$x_\mu = [\mu_{x1}, \mu_{x2}, \ldots, x_{t,i}, \ldots, \mu_{xm}] \quad (44)$$

11- Determining the response weighting factor of the IPL energy planning algorithm step 10:

$$w_0 = 1 - \sum_{t=1}^{m} \frac{1}{\lambda_{t,4}-\lambda_{t,3}^2} \quad (45)$$

12- Update E(Yj):

$$E(Y^j) = E(Y^j) + w_0[F(X^\mu)] \quad (46)$$

$$E(Y^j) = \sum_{t=1}^{m}\sum_{i=1}^{2} w_{ti}[F(\mu_{x1}, \mu_{x2}, \ldots, x_{t,i}, \ldots, \mu_{xm})]^j + w_0[F(X^\mu)] \quad (47)$$

By knowing the statistical moments of the output random variable, the mean and standard deviation can be calculated:

$$\mu_Y = E(Y) \quad (48)$$
$$\sigma_Y = \sqrt{E(Y^2) - \mu_Y^2} \quad (49)$$

Based on the statistical moments, the probability density functions of the desired output random variables can be approximated using the Gram-Charlier series method.

4.2. Information-Gap Decision Theory (IGDT)

Due to limitations in current prediction methods, smart parking operators must calculate their own estimates associated with inherent uncertainties related to predicted variables such as wind speed, solar radiation, and demand. These uncertainties can significantly impact decision-making processes regarding IPL performance for the next day. To address this issue, an appropriate method for modeling these uncertainties is necessary. The method used in this study is the Information-Gap Decision Theory (IGDT). IGDT is a non-probabilistic approach designed for managing models with uncertain input data. This method enhances uncertainty radius, provides a solution, and offers specific expectations regarding the target variable. IGDT consists of two main strategies: RA-IGDT and RS-

IGDT[39].

- **Risk-Averse Strategy RA-IGDT:** This strategy is employed when the uncertainty associated with a non-certain parameter negatively affects the objective function of the problem. In essence, the realization of the uncertain parameter should lead to an increase in the objective function from its baseline value. Therefore, the RA-IGDT strategy aims to identify the maximum uncertainty radius for the non-certain parameter, considering a specific predetermined level of objective function degradation from its baseline value. This approach involves determining optimal values for decision variables that maximize the uncertainty radius for the non-certain parameter, allowing for a specific increase in the objective function.

- **Risk-Seeking Strategy RS-IGDT:** The RS-IGDT strategy is used when uncertainty associated with a non-certain parameter does not always lead to objective function degradation. In this strategy, the realization of the non-certain parameter not only has no negative effect on the objective function but also reduces it from its baseline value. Essentially, decision-makers in this strategy seek to achieve a lower objective function than the baseline value due to positive changes in the uncertain parameter.

4.2.1. RA-IGDT

In the Risk-Averse strategy, decision-making regarding problem variables is performed in a way that makes the problem resistant to undesirable changes in uncertain parameters. In other words, in the risk-averse strategy, the system designer reduces the risk and ensures that, in the event of undesirable changes in non-certain parameters, the objective function will not exceed a virtual threshold set to determine the uncertainty radius of the non-certain parameter[40,41].

$$Max\ \alpha$$
$$\forall X \in U(\alpha, \bar{X})$$
$$f(X, d) \leq l_c$$
$$l_c = f_b(X, d) \times (1 + \beta)$$
$$H_i(\bar{X}, d) = \cdot, \forall i \in \Omega_I$$
$$G_j(\bar{X}, d) \geq \cdot, \forall j \in \Omega_E \qquad (50)$$
$$0 \leq \beta \leq 1$$

In the above equations, l_c represents the critical value of the objective function, which is usually determined by the decision-maker. Additionally, β is the coefficient of maximum deviation from the baseline value of the objective function, which is determined by the operator.

5. Numerical Results

.

In this section, numerical results related to the planning and optimal management of IPL using the combined D-BHA method are evaluated. In addition to the results concerning IPL energy management, optimal optimization results for nine standard test functions are provided in the appendix to demonstrate the superior performance of the combined algorithm. According to the optimization results, the performance of the combined D-HBA algorithm has been better, and therefore, only this algorithm has been utilized in simulations related to IPL.

5.1. System Under Study

The scheduling of electric vehicle (EV) charging and discharging with the aim of maximizing parking revenue and minimizing costs for EV owners, reducing green certification costs and pollution emissions, as well as adhering to technical, economic constraints, and penalties related to charge compliance and cost thresholds, constitutes the main components of this study. Considering the investment and utilization of parking lots and associated resources, this study has been fully explained. The planned parking infrastructure is illustrated in Fig. 2. The interaction between IPL and the upstream network, as well as energy storage systems and renewable energy sources, is depicted in this image. This IPL participates in the future market (at the distribution market level), and IPL management is responsible for energy exchange with the upstream network. A fuel cell, an electrolyzer, and a hydrogen storage tank constitute the hydrogen storage system.
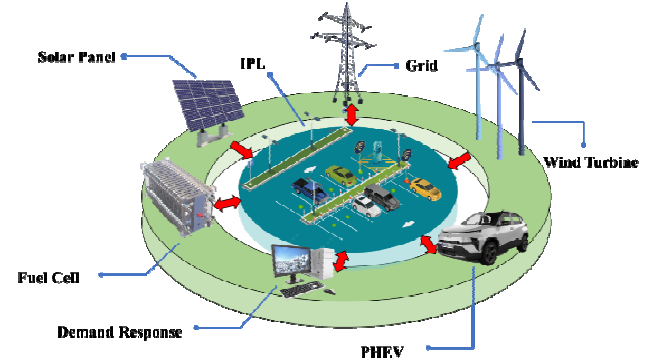
Fig. 2. Proposed IPL topology with equipment.

Renewable energy sources are wind turbines and photovoltaic sources, each with a capacity of 30 kW, as indicated in Table 1. The hydrogen storage system includes electrolysis, FC, and hydrogen storage tank, whose technical specifications are given in Table 2 and Table 3. In the studied system, there are 10 V2G units capable of both charging and discharging and 5 G2V units participating in the IPL throughout the day.

Table 1. PV system and wind turbine unit parameters[32,42].

	PV system			Wind turbine	
Parameters	Value	Unit	parameters	Value	unit
R	1	kW/m2	VC	3	m/s
			VR	12	m/s
T	25	˚c	VF	30	m/s

Table 2. Technical specifications of the hydrogen unit [32].

PEL-max kW	PFC-max kW	MTank-max Kg	MTank-min kg	MTank-initial kg	EH2 kWh/kg
40	20	8	1.25	5	39.7

Table 3. Equipment's economic attributes[32].

Components	Maintenance costs Cm $/year	Capacity factor CF %	Initial investment cost A $/W	Life time n Year	Efficiency %
Hydrogen tank	20	0.9	0.625	15	95
Fuel cell	13	0.9	0.700	20	50
Electrolyzer	15	0.9	0.350	25	75

All PHEVs utilized in this examination shared identical specifications. The technical details of these PHEVs are outlined in Table 4. Each PHEV is assumed to have a maximum power consumption of 4 kilowatts for both charging and discharging purposes. Table 5 presents the rates for charging and discharging, available capacity, and penalty rates applicable V2G vehicles, alongside the charging and discharging costs for G2V vehicles. Additionally, Table 6 exhibits the anticipated SOC of V2G vehicles upon departure. Tables 7 and 8 furnish projections for departure and arrival times, as well as the initial SOC of the vehicles. In Table 9, the information related to the cost of responding to the load according to the percentage of the load ratio is given.

Table 4. Technical specifications of PHEVs[27,32].

PHEV	Battery Lithium-Ion kWh	η_c^v %	η_d^v %	SOCmin %	SOCmax %
NISSAN LEAF	24	90	95	15	95

Table 5. PHEV charging and discharging tariff [27,32].

ρ_c^t $/kWh	$\rho_{c \cdot V2G}^t$ $/ kWh	$\rho_{d,V2G}^t$ $/ kWh	$\rho_{cap.V2G}^t$ $/ kWh	$\rho_{penalty}$ $/ kWh
1.3* ρ_{grid}^t	1.1* $\rho_v^{Plug-in}$	1* $\rho_v^{Plug-in}$	0.02* $\rho_v^{Plug-in}$	4* $\rho_v^{Plug-in}$

*$\rho_v^{Plug-in}$ is the market price on average for the number of times each PHEV is connected.

Table 6. Desired SOC of PHEV V2G [27,32]

PHEV (v)	1	2	3	4	5	6	7	8	9	10
SOC_v^{desi}	90	60	90	85	75	75	55	70	90	60

Table 7. PHEVs' predicted G2V data [27,32].

PHEV(v)	t_v^a	t_v^d	$SOC_v^{t_d}$
1	7:13	13:11	45.59
2	9:10	15:20	22.04
3	9:35	15:50	27.3
4	7:35	18:50	40.36
5	12:07	21:45	16.47

Table 8. Predicted data of PHEV V2Gs [27,32].

PHEV (v)			
1	7:10	15:33	50
2	8:55	17:55	31.6
3	6:20	15:25	42.9
4	8:12	16:43	48.2
5	8:05	13:46	42.5
6	7:46	17:05	37.8
7	9:55	13:40	48.5
8	5	16:30	33
9	6:10	14:40	63
10	7:42	13:50	46.3

Table 9. Data related to demand response [43]

Load	33%	66%	100%
DR Cost (kW/$)	2.5	3.5	4.5

The characteristics of the predicted market price and load demand values are shown in Fig. 3. $\rho_{\text{sell-load}}^{t}$ tariff is 30% higher than the market price. The amount of solar radiation and wind speed are also shown in Fig. 4.
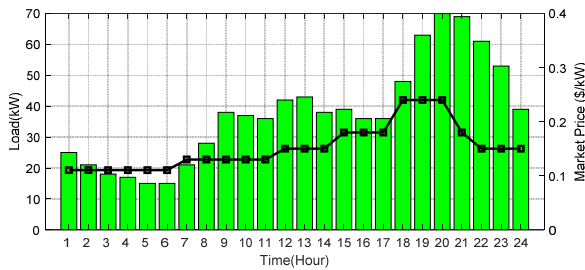
Fig. 3. Market price and predicted cargo demand [50].
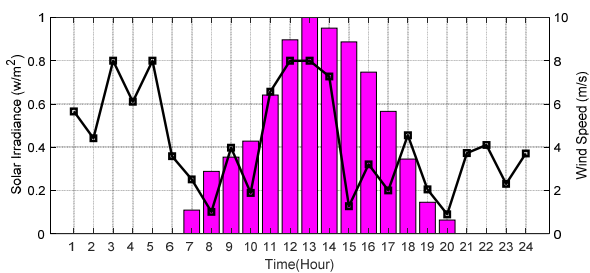
Fig. 4. Predicted wind speed and solar radiation.

5.2. Simulation Results

This section presents the results obtained from optimizing the proposed model using the DHBA optimization algorithm. To this end, the proposed model for optimizing the performance of Intelligent Parking Lots (IPL) using MATLAB software was solved on a personal computer with an Intel Core i5-4460 CPU @ 3.20GHz and 12 gigabytes of RAM. To better evaluate the optimized performance of IPL, three simulation scenarios have been considered. These scenarios are summarized as follows:

- Scenario 1: Optimization of IPL without considering demand response and green certificates deterministically.
- Scenario 2: Optimization of IPL considering demand response and green certificates deterministically.
- Scenario 3: Optimization of IPL considering demand response and green certificates probabilistically.

Subsequently, the results of each scenario are discussed and analyzed.

5.2.1. Scenario 1

To evaluate the performance of the proposed IPL model in this scenario, energy management strategies were implemented using the real IPL model. The objective of this scenario is to assess the optimized performance of IPL without considering the uncertainty of renewable sources and the dynamic nature of load and renewable resources. Additionally, demand response and green certificate costs are not taken into account in this scenario. The simulation was conducted using a deterministic approach and provided valuable insights into the effectiveness of the proposed strategy. The problem of optimizing IPL performance in the presence of renewable sources was solved using the proposed optimization method.

In this scenario, the aim is to examine the effects of wind and solar renewable sources. These sources interact with other components in IPL to determine an optimal scheduling of unit production and charge/discharge of units and vehicles. The results obtained from optimization using the DHBA algorithm are presented in Table 10. These findings indicate that the profit obtained has increased compared to the scenario where renewable sources are absent, amounting to $2103.1 thousand. This result demonstrates the effectiveness of the optimization method in optimizing revenues against costs.

The visual results of optimization are illustrated in Fig.s 5 through 7. Fig. 5 depicts the optimized scheduling and power interactions among different sections of IPL in the presence of renewable sources. It is observed that the purchased power from the grid is mostly utilized for charging V2G vehicles during off-peak hours, while renewable sources contribute the highest share of power during these hours. Additionally, in some instances, power is sold back to the grid during hours 5 and 6, corresponding to lower demand periods, leading to increased system profits.

The variations in hydrogen mass resulting from power exchange are illustrated in Fig. 6, indicating that hydrogen mass stored in the tank is injected into IPL via fuel cells

during hours 1-8 and 17-24, while it begins to be stored through various sources between hours 8 and 17. The presence of fuel cells as green storage reduces the reliance on grid-supplied power during times when renewable sources, such as photovoltaic, have zero power output.

Fig. 7 illustrates the power for charging and the number of G2V charged and the power for V2G charge/discharge over time. In this scenario, power during hours 8-17 is primarily supplied through renewable sources, utilizing stored power in HSS and power derived from V2G discharge in IPL, as shown in Fig. 7.

The optimal interaction between exchanged power in various units at different times has facilitated the effective provision of loads and fulfilled all problem constraints, ultimately resulting in cost reduction and profit increase.
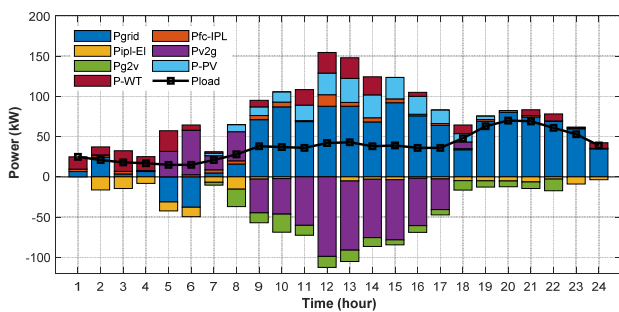
Fig. 5. IPL power planning and management (Scenario 1).
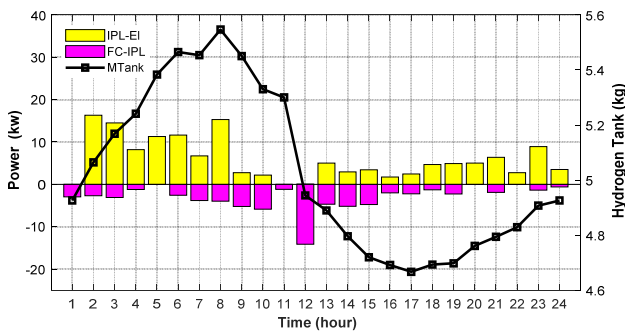
Fig.6. Scheduling of fuel cell power along with hydrogen tank capacity (scenario 1).
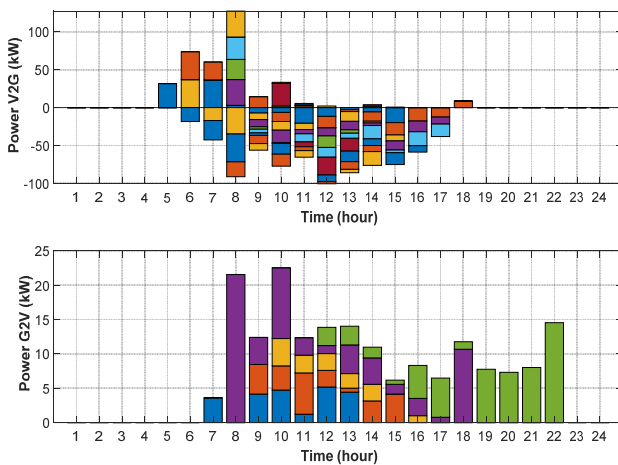
Fig.7. Scheduling V2G charging and discharging along with G2V power in IPL (Scenario 1).

Table 10. Optimal results of IPL energy management, costs and income (scenario 1)

Parameter	Value
Revenue of Grid ($)	1.89541×10^2
Revenue of Load ($)	1.65321×10^2
Revenue of V2G ($)	1.50760×10^2
Revenue of G2V ($)	84.9627×10^1
Cost of V2G ($)	2.59191×10^2
Cost of FC ($)	5.31033×10^2
Cost of Electrolyzer ($)	6.25516×10^2
Cost of Tank ($)	4.03987×10^2
Cost of REN ($)	4.56342×10^2
Profit ($)	2.10308×10^4

5.2.2. Scenario 2

In this scenario, the integration of renewable sources and demand response, along with considering the costs of green certificate issuance, demonstrates a significant transformation in IPL's energy management strategy. The strategic integration of renewable sources, as depicted in Fig. 8, emphasizes IPL's commitment to sustainable energy practices by optimizing the use of solar and wind energy while meeting fluctuating load demands. This strategic integration not only reduces reliance on non-renewable energy sources but also aligns with IPL's environmental objectives. According to the results, during hours 9 to 17, the highest power for G2V is mainly supplied from V2G vehicles, renewable sources, and other sources with an additional share from fuel cells. This strategic energydistribution ensures efficient utilization of available resources and minimizes resource wastage.

Additionally, considering demand response, as shown in Fig.s 8 and 11, enables IPL to dynamically adjust its power scheduling and management, ensuring efficient resource utilization and minimizing wastage. This adaptability enhances the overall system performance and flexibility in response to changing demand patterns. Moreover, incorporating the costs of green certificate issuance, as depicted in Table 11, indicates IPL's environmental stewardship and willingness to invest in sustainable practices. While these costs may impact operational expenses, they contribute to IPL's significance as an environmentally conscious system.

Based on the results, efficient scheduling of fuel cell power management and hydrogen storage tank capacity, as illustrated in Fig. 9, ensures a reliable and continuous power supply, optimizing energy efficiency and minimizing resource wastage. Similarly, strategic planning of V2G charge and discharge, as shown in Fig. 10, utilizes electric vehicles as mobile energy storage units, providing additional revenue streams and contributing to grid stability.

Additionally, the variations in stored hydrogen mass in the tank indicate that from hour 10 to 17, there is a greater accumulation of hydrogen mass coinciding with peak demand periods. This pattern reflects a strategic shift in fuel cell usage, alignment with peak demand periods, and maximizing energy storage and distribution efficiency.

Overall, Scenario 2 serves as an exemplar of IPL's comprehensive approach to energy management, balancing financial profitability with environmental sustainability and social responsibility. In this scenario, profits increase to $24,905.3, indicating a significant improvement compared to Scenario 1 ($21,030.8), representing an approximate 18.5% increase.
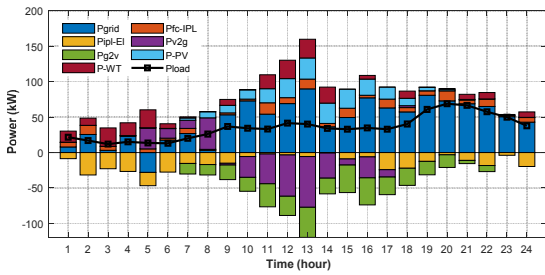
Fig.8. IPL power planning and management (Scenario 2).
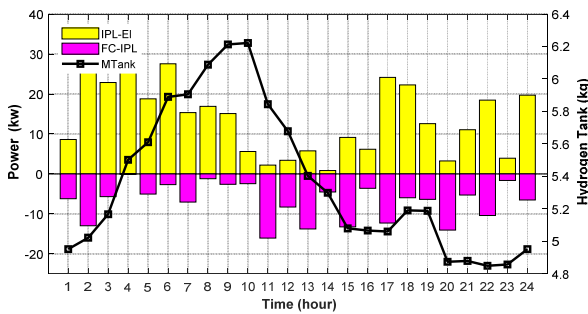
Fig.9. Scheduling of fuel cell power along with hydrogen tank capacity (Scenario 2).
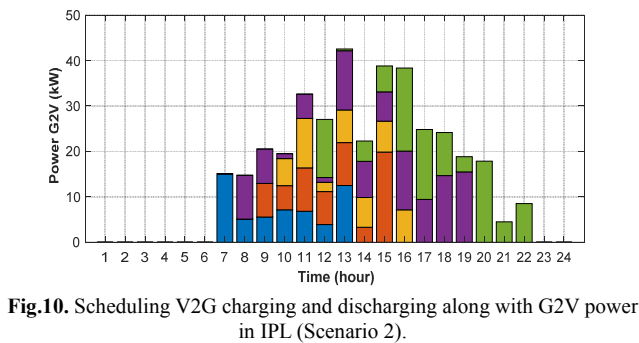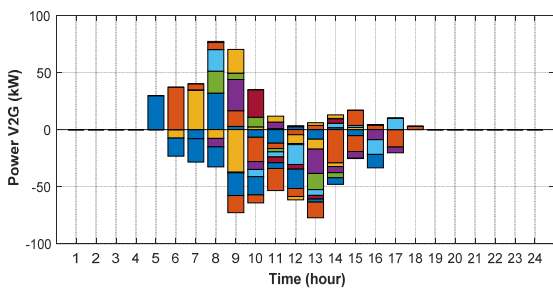
Fig.10. Scheduling V2G charging and discharging along with G2V power in IPL (Scenario 2).
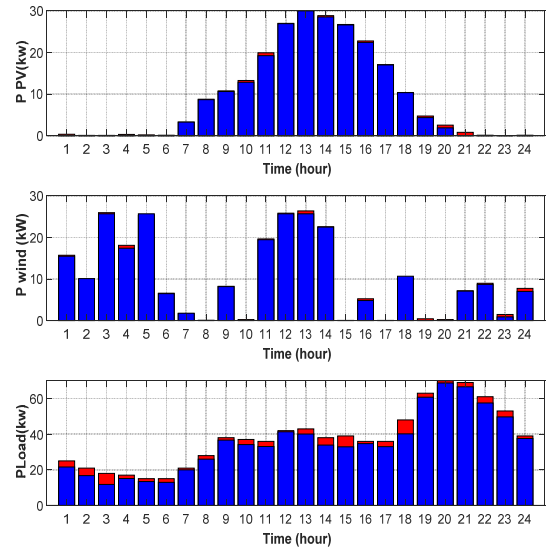
Fig.11. Solar-wind power production plan and load response (Scenario 2)

Table 11. Optimal results of IPL energy management, costs and income (Scenario 2)

Parameter	Value
Revenue of Grid ($)	1.82905×10^2
Revenue of Load ($)	1.53421×10^2
Revenue of V2G ($)	1.00975×10^2
Revenue of G2V ($)	36.4463×10^1
Cost of V2G ($)	33.1330×10^2
Cost of FC ($)	5.97857×10^2
Cost of Electrolyzer ($)	6.58928×10^2
Cost of Tank ($)	4.63745×10^2
Cost of REN ($)	4.66046×10^2
Cost of DR ($)	3.05433×10^2
Cost of GC ($)	4.95060×10^2
Profit ($)	2.49053×10^4

5.2.3. Scenario 3

Given the intermittent nature of renewable power generation and demand variations, this section examines the impact of uncertainty in these sources and load demand. To this end, a combined approach of two-piecewise estimation method and Risk-Averse Integrated Green Decision Theory (TPEM-RAIGDT) has been employed to model uncertainty. Initially, the TPEM method is used to obtain probabilistic data for wind, solar, and load, followed by the RAIGDT method to determine the uncertainty radius using the DHBA optimization method. Unlike the Monte Carlo

method, this approach requires fewer samples and a single uncertainty radius to model uncertainty effectively. Additionally, due to the probabilistic nature of the input data, the uncertainty radius is asymmetric and probabilistic.

Fig. 11 illustrates the data generated for each of the renewable sources and load using the TPEM method. The values obtained from this method are shown to have a narrower range compared to predicted data. The energy management of IPL is optimized for each data point using the generated data from this method. Finally, statistical parameters such as mean and standard deviation are calculated for this method.

The optimization results in this scenario for different β values based on the profit obtained from Scenario 2 are presented in Table 12. It can be observed that profit decreases with an increase in the uncertainty radius. Moreover, the changes in the uncertainty radius and profit are illustrated in Fig. 13. Additionally, considering the uncertainty reduces the profit compared to the deterministic optimization scenario, attributed to the consideration of non-deterministic conditions of sources and load.

To select an appropriate uncertainty radius with reasonable and acceptable profit margins, a β value of 1.5%is chosen. After optimization, the results obtained are presented in Table 13. In this case, the profit value is $2.25126 thousand, which indicates a decrease of a few percentage points compared to the deterministic scenario.

Furthermore, the simulation results of Scenario 3 in Fig. 14 depict the optimized energy management and interactions of IPL components with the grid. It is evident from Fig. 14 that due to renewable energy generation, purchasing decreases in some time periods. This reduction in purchasing from the grid coincides with an increase in stored hydrogen mass in the tank, facilitating consumption during peak demand hours. The presence of this source and the possibility of energy storage and direct consumption in hydrogen fuel cell electric vehicles will have the greatest economic benefit for IPL owners. Thus, IPL management with system uncertainty can provide practical applications with similar economic benefits to Scenario 2. Additionally, at hour 3, despite the presence of renewable sources, selling to the grid occurs, leading to increased profit. However, compared to Scenario 2, grid purchasing increases in more instances due to uncertainty, resulting in a decrease in energy purchase income.

Fig. 15 illustrates changes in hydrogen tank mass and power exchanges between HSS and IPL. With increased purchasing from the grid and interactions with electric vehicles, the amount of energy stored in the hydrogen tank increases during early and low-demand hours. However, due to uncertainty regarding electric vehicle loads and storage benefits, this increases the cost of HSS.

Fig. 16 also depicts changes in the power and participation levels of G2V and V2G. As seen in these figures, the total charge and discharge power of these electric vehicles decrease compared to Scenario 2 based on charge and discharge management decisions. Additionally, a comparison of the two scenarios reveals that the number

of vehicles involved in the charging and discharging process changes slightly, and even remains equal in some hours. However, due to the uncertain system, the charging and discharging capacity of each EV has changed.

Fig. 17 also illustrates changes in wind and solar generation considering the cost of green certificates, along with the participation levels of loads in the demand response program.
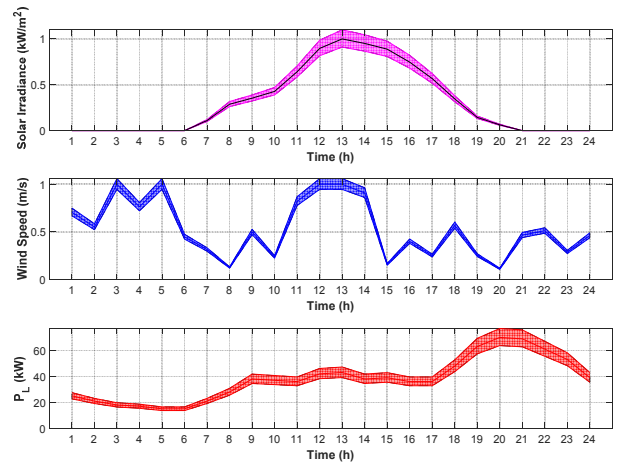
Fig.12. Uncertainty range of solar radiation and wind speed using point estimation method (scenario 3)
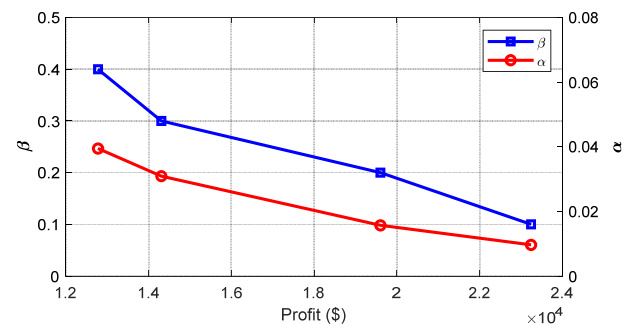
Fig.13. Uncertainty radius according to β changes based on profit (scenario 3)
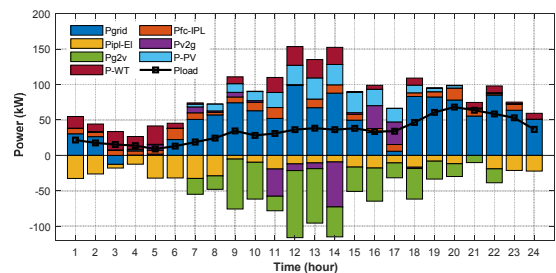
Fig. 14. IPL power planning and management (Scenario 3)
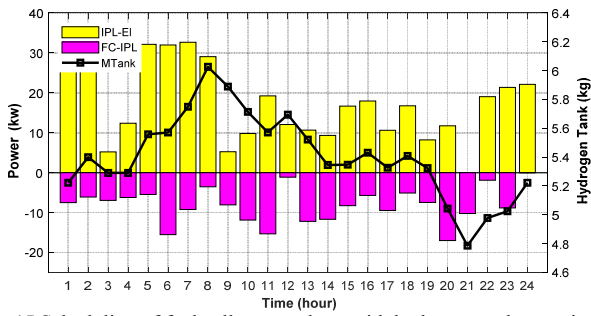
Fig.15. Scheduling of fuel cell power along with hydrogen tank capacity (scenario 3)

Table 12. Results of the combined TPEM-RAIGDT method for the radius of uncertainty (scenario 3)

β	α	Profit ($)
0.1	0.00964	2.21435×10^4
0.2	0.01568	1.96029×10^4
0.3	0.03092	1.43082×10^4
0.4	0.03946	1.27773×10^4
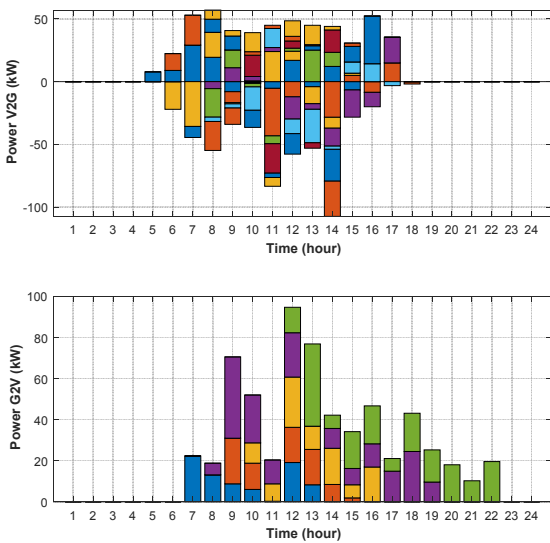
Fig.16. Scheduling V2G charging and discharging along with G2V power in IPL (scenario 3)

Table 13. Optimal results of IPL energy management, costs and income (scenario 3)

Parameter	Value
Revenue of Grid ($)	1.80721×10^2
Revenue of Load ($)	1.56225×10^2
Revenue of V2G ($)	1.09405×10^2
Revenue of G2V ($)	1.59372×10^2
Cost of V2G ($)	1.44884×10^2
Cost of FC ($)	3.97728×10^2
Cost of Electrolyzer ($)	6.04085×10^2
Cost of Tank ($)	6.62042×10^2
Cost of REN ($)	4.68409×10^2
Cost of DR ($)	2.46510×10^2
Cost of GC ($)	1.37915×10^3
Profit ($)	2.25126×10^4

5.3. Comparison of Results

After a thorough analysis of the three potential scenarios with the aim of increasing the efficiency of IPL management and utilizing the DHBA optimization method, significant findings regarding the practicality and benefits of the proposed strategy have emerged. This underscores its implementability in real-world environments, especially in smart parking facilities. Through comprehensive examination using both deterministic and probabilistic approaches, a comprehensive understanding of the optimal exploitation framework of IPL has been achieved. This includes various aspects such as vehicle charging and discharging, upstream network purchasing, hydrogen storage, demand response, green certification, pollution emission, and electrolysis performance under different conditions, whether usual or uncertain.

The cost and income results for each of the three scenarios are precisely presented in Table 14. Upon reviewing these findings, it is evident that the integration of renewable sources leads to increased profitability. It also

Fig.17. Solar-wind power generation plan and demand response (scenario 3)

reduces environmental impacts and pollution emissions by maximizing renewable resources. However, on the other hand, calculating uncertainties using the proposed combined method results in reducing profit margins. Consequently, IPL operators can make informed decisions to maintain reasonable profit margins and ensure optimal and beneficial exploitation facilitation.

Table 14. Optimal results of IPL energy management, costs and income

Parameter	scenario 1	scenario 2	scenario 3
Revenue of Grid ($)	1.89541×10^2	1.82905×10^2	1.80721×10^2
Revenue of Load ($)	1.65321×10^2	1.53421×10^2	1.56225×10^2
Revenue of V2G ($)	1.50760×10^2	1.00975×10^2	1.09405×10^2
Revenue of G2V ($)	84.9627×10^1	36.4463×10^1	1.59372×10^2
Cost of V2G ($)	2.59191×10^2	33.1330×10^2	1.44884×10^2
Cost of FC ($)	5.31033×10^2	5.97857×10^2	3.97728×10^2
Cost of Electrolyzer ($)	6.25516×10^2	6.58928×10^2	6.04085×10^2
Cost of Tank ($)	4.03987×10^2	4.63745×10^2	6.62042×10^2
Cost of REN ($)	4.56342×10^2	4.66046×10^2	4.68409×10^2
Cost of DR ($)	--	3.05433×10^2	2.46510×10^2
Cost of GC ($)	--	4.95060×10^2	1.37915×10^3
Profit ($)	2.10308×10^4	2.49053×10^4	2.25126×10^4

6. Conclusion

The integration of Intelligent Parking Lots (IPLs) with Renewable Energy Sources (RES) and Hydrogen Storage Systems (HSS) holds significant promise in achieving both technical and environmental objectives. This paper proposes a novel energy management framework for IPLs based on HSS, encompassing various energy management strategies. Our analyses demonstrate that these systems, by leveraging diverse energy management approaches and clean energy sources, can achieve high profitability and desirable performance. Moreover, considering uncertainty and employing combined modeling methods can enhance system performance under different conditions. These findings indicate that IPL operators, through cautious decision-making, can minimize costs while simultaneously increasing system profitability, leading to efficient and effective operations.

The adoption of integrated solutions of smart electric parking combined with renewable energy sources and hydrogen storage systems can play a crucial role in addressing the growing demand for sustainable energy solutions. By employing advanced energy management strategies and utilizing renewable energy sources, these systems have the potential to reduce carbon emissions and reliance on traditional energy grids. Furthermore, the integration of hydrogen storage systems enables efficient energy storage and utilization, enhancing overall infrastructure sustainability and flexibility. Additionally, our study underscores the importance of considering uncertainty and employing robust modeling techniques to calculate various factors affecting system performance. By combining probabilistic modeling and decision frameworks, IPL operators can better anticipate and mitigate risks associated with energy management and resource utilization. This proactive approach not only enhances system efficiency but also ensures adaptability and flexibility in facing variable environmental conditions and operations. In conclusion, the findings highlight the transformative potential of integrating renewable energy sources and hydrogen storage systems in electric parking lots. Through strategic planning and effective management practices, IPL operators can optimize system performance, minimize costs, maximize profitability, and ultimately contribute to the creation of a more sustainable and resilient urban energy infrastructure.

Reference

[1]   I.F. Davoudkhani, A. Dejamkhooy, S.A. Nowdeh, A novel cloud-based framework for optimal design of stand-alone hybrid renewable energy system considering uncertainty and battery aging, Appl Energy 344 (2023) 121257. https://doi.org/10.1016/J.APENERGY.2023.121257.

[2]   M. Alinejad, O. Rezaei, A. Kazemi, S. Bagheri, An Optimal Management for Charging and Discharging of Electric Vehicles in an Intelligent Parking Lot Considering Vehicle Owner's Random Behaviors, J Energy Storage 35 (2021) 102245. https://doi.org/10.1016/J.EST.2021.102245.

[3]   P. Zare, A. Dejamkhooy, I.F. Davoudkhani, Efficient expansion planning of modern multi-energy distribution networks with electric vehicle charging stations: A stochastic MILP model, Sustainable Energy, Grids and Networks 38 (2024) 101225. https://doi.org/10.1016/J.SEGAN.2023.101225.

[4]   M. Yazdani-Damavandi, M.P. Moghaddam, M.-R. Haghifam, M. Shafie-khah, J.P.S. Catalao, Modeling Operational Behavior of Plug-in Electric Vehicles' Parking Lot in Multienergy Systems,

IEEE Trans Smart Grid 7 (2016) 124–135. https://doi.org/10.1109/TSG.2015.2404892.

[5]   S. Arabi Nowdeh, A. Naderipour, I. Faraji Davoudkhani, J.M. Guerrero, Stochastic optimization – based economic design for a hybrid sustainable system of wind turbine, combined heat, and power generation, and electric and thermal storages considering uncertainty: A case study of Espoo, Finland, Renewable and Sustainable Energy Reviews 183 (2023) 113440. https://doi.org/10.1016/J.RSER.2023.113440.

[6]   A.F. Marzoghi, S. Bahramara, F. Adabi, S. Nojavan, Interval multi-objective optimization of hydrogen storage based intelligent parking lot of electric vehicles under peak demand management, J Energy Storage 27 (2020) 101123. https://doi.org/10.1016/J.EST.2019.101123.

[7]   A. El-Zonkoly, L. dos Santos Coelho, Optimal allocation, sizing of PHEV parking lots in distribution system, International Journal of Electrical Power & Energy Systems 67 (2015) 472–477. https://doi.org/10.1016/J.IJEPES.2014.12.026.

[8]   M. Mojarad, M. Sedighizadeh, M. Dosaranian☐Moghadam, Optimal allocation of intelligent parking lots in distribution system: A robust two☐stage optimization model, IET Electrical Systems in Transportation 12 (2022) 102–127. https://doi.org/10.1049/els2.12042.

[9]   M.A. Baherifard, R. Kazemzadeh, A.S. Yazdankhah, M. Marzband, Intelligent charging planning for electric vehicle commercial parking lots and its impact on distribution network's imbalance indices, Sustainable Energy, Grids and Networks 30 (2022) 100620. https://doi.org/10.1016/J.SEGAN.2022.100620.

[10]   M. Tostado-Véliz, A.R. Jordehi, S.A. Mansouri, F. Jurado, A two-stage IGDT-stochastic model for optimal scheduling of energy communities with intelligent parking lots, Energy 263 (2023) 126018. https://doi.org/10.1016/J.ENERGY.2022.126018.

[11]   L. Zhang, D. Liu, G. Cai, L. Lyu, L.H. Koh, T. Wang, An optimal dispatch model for virtual power plant that incorporates carbon trading and green certificate trading, International Journal of Electrical Power & Energy Systems 144 (2023) 108558. https://doi.org/10.1016/J.IJEPES.2022.108558.

[12]   W. Chang, Q. Yang, Low carbon oriented collaborative energy management framework for multi-microgrid aggregated virtual power plant considering electricity trading, Appl Energy 351 (2023) 121906. https://doi.org/10.1016/j.apenergy.2023.121906.

[13]   V. Saini, S. Tiwari, G.N. Tiwari, Environ economic analysis of various types of photovoltaic technologies integrated with greenhouse solar drying system, J Clean Prod 156 (2017) 30–40. https://doi.org/10.1016/J.JCLEPRO.2017.04.044.

[14]   H. Mikulčić, M. Vujanović, K. Urbaniec, N. Duić, Reducing greenhouse gasses emissions by fostering the deployment of alternative raw materials and energy sources in the cleaner cement manufacturing process, J Clean Prod 136 (2016) 119–132. https://doi.org/10.1016/J.JCLEPRO.2016.04.145.

[15]   C.G. Hoehne, M. V. Chester, Optimizing plug-in electric vehicle and vehicle-to-grid charge scheduling to minimize carbon emissions, Energy 115 (2016) 646–657. https://doi.org/10.1016/J.ENERGY.2016.09.057.

[16]   M.-K. Kim, J. Oh, J.-H. Park, C. Joo, Perceived value and adoption intention for electric vehicles in Korea: Moderating effects of environmental traits and government supports, Energy 159 (2018) 799–809. https://doi.org/10.1016/J.ENERGY.2018.06.064.

[17]   J. Jannati, D. Nazarpour, Optimal performance of electric vehicles parking lot considering environmental issue, J Clean Prod 206 (2019) 1073–1088. https://doi.org/10.1016/J.JCLEPRO.2018.09.222.

[18]   S. Khan, A. Ahmad, F. Ahmad, M. Shafaati Shemami, M. Saad Alam, S. Khateeb, A Comprehensive Review on Solar Powered Electric Vehicle Charging System, Smart Science 6 (2018) 54–79. https://doi.org/10.1080/23080477.2017.1419054.

[19]   E. Yoo, M. Kim, H.H. Song, Well-to-wheel analysis of hydrogen fuel-cell electric vehicle in Korea, Int J Hydrogen Energy 43 (2018) 19267–19278. https://doi.org/10.1016/J.IJHYDENE.2018.08.088.

[20]   A. Mazzucco, M. Dornheim, M. Sloth, T.R. Jensen, J.O. Jensen, M. Rokni, Bed geometries, fueling strategies and optimization of heat exchanger designs in metal hydride storage systems for automotive applications: A review, Int J Hydrogen Energy 39 (2014) 17054–17074. https://doi.org/10.1016/J.IJHYDENE.2014.08.047.

[21]   M. Ghiyasiyan-Arani, M. Salavati-Niasari, Effect of Li 2 CoMn 3 O 8 Nanostructures Synthesized by a Combustion Method on Montmorillonite K10 as a Potential Hydrogen Storage Material, The Journal of Physical Chemistry C 122 (2018) 16498–16509. https://doi.org/10.1021/acs.jpcc.8b02617.

[22]   A. Salehabadi, M. Salavati-Niasari, T. Gholami, Green and facial combustion synthesis of Sr3Al2O6 nanostructures; a potential electrochemical hydrogen storage material, J Clean Prod 171 (2018) 1–9. https://doi.org/10.1016/J.JCLEPRO.2017.09.250.

[23]   J. Guo, Y. Lv, H. Zhang, S. Nojavan, K. Jermsittiparsert, Robust optimization strategy for intelligent parking lot of electric vehicles, Energy 200 (2020) 117555. https://doi.org/10.1016/J.ENERGY.2020.117555.

[24]   M.H. Amini, M.P. Moghaddam, O. Karabasoglu, Simultaneous allocation of electric vehicles'

parking lots and distributed renewable resources in smart power distribution networks, Sustain Cities Soc 28 (2017) 332–342. https://doi.org/10.1016/J.SCS.2016.10.006.

[25] K. Seddig, P. Jochem, W. Fichtner, Integrating renewable energy sources by electric vehicle fleets under uncertainty, Energy 141 (2017) 2145–2153. https://doi.org/10.1016/J.ENERGY.2017.11.140.

[26] M. Honarmand, A. Zakariazadeh, S. Jadid, Self-scheduling of electric vehicles in an intelligent parking lot using stochastic optimization, J Franklin Inst 352 (2015) 449–467. https://doi.org/10.1016/J.JFRANKLIN.2014.01.019.

[27] R. Razipour, S.-M. Moghaddas-Tafreshi, P. Farhadi, Optimal management of electric vehicles in an intelligent parking lot in the presence of hydrogen storage system, J Energy Storage 22 (2019) 144–152. https://doi.org/10.1016/J.EST.2019.02.001.

[28] M. Honarmand, A. Zakariazadeh, S. Jadid, Integrated scheduling of renewable generation and electric vehicles parking lot in a smart microgrid, Energy Convers Manag 86 (2014) 745–755. https://doi.org/10.1016/J.ENCONMAN.2014.06.044.

[29] M.S. Kuran, A. Carneiro Viana, L. Iannone, D. Kofman, G. Mermoud, J.P. Vasseur, A Smart Parking Lot Management System for Scheduling the Recharging of Electric Vehicles, IEEE Trans Smart Grid 6 (2015) 2942–2953. https://doi.org/10.1109/TSG.2015.2403287.

[30] M. Honarmand, A. Zakariazadeh, S. Jadid, Optimal scheduling of electric vehicles in an intelligent parking lot considering vehicle-to-grid concept and battery condition, Energy 65 (2014) 572–579. https://doi.org/10.1016/J.ENERGY.2013.11.045.

[31] L. Zhang, Y. Li, A Game-Theoretic Approach to Optimal Scheduling of Parking-Lot Electric Vehicle Charging, IEEE Trans Veh Technol 65 (2016) 4068–4078. https://doi.org/10.1109/TVT.2015.2487515.

[32] S. Kashiri, J. Siahbalaee, A. Koochaki, Stochastic management of electric vehicles in an intelligent parking lot in the presence of hydrogen storage system and renewable resources, Int J Hydrogen Energy 50 (2024) 1581–1597. https://doi.org/10.1016/J.IJHYDENE.2023.10.146.

[33] S. Arabi Nowdeh, I.F. Davoudkhani, M.J. Hadidian Moghaddam, E.S. Najmi, A.Y. Abdelaziz, A. Ahmadi, S.E. Razavi, F.H. Gandoman, Fuzzy multi-objective placement of renewable energy sources in distribution system with objective of loss reduction and reliability improvement using a novel hybrid method, Appl Soft Comput 77 (2019) 761–779. https://doi.org/10.1016/J.ASOC.2019.02.003.

[34] S. Zhang, W. Hu, X. Cao, J. Du, C. Bai, W. Liu, M. Tang, W. Zhan, Z. Chen, Low-carbon economic dispatch strategy for interconnected multi-energy microgrids considering carbon emission accounting and profit allocation, Sustain Cities Soc 99 (2023) 104987. https://doi.org/10.1016/J.SCS.2023.104987.

[35] F.A. Hashim, E.H. Houssein, K. Hussain, M.S. Mabrouk, W. Al-Atabany, Honey Badger Algorithm: New metaheuristic algorithm for solving optimization problems, Math Comput Simul 192 (2022) 84–110. https://doi.org/10.1016/J.MATCOM.2021.08.013.

[36] F. Huang, L. Wang, Q. He, An effective co-evolutionary differential evolution for constrained optimization, Appl Math Comput 186 (2007) 340–356. https://doi.org/10.1016/J.AMC.2006.07.105.

[37] Juan.M. Morales, Juan. Perez-Ruiz, Point Estimate Schemes to Solve the Probabilistic Power Flow, IEEE Transactions on Power Systems 22 (2007) 1594–1601. https://doi.org/10.1109/TPWRS.2007.907515.

[38] C.-L. Su, Probabilistic Load-Flow Computation Using Point Estimate Method, IEEE Transactions on Power Systems 20 (2005) 1843–1851. https://doi.org/10.1109/TPWRS.2005.857921.

[39] T. Sriyakul, K. Jermsittiparsert, Economic scheduling of a smart microgrid utilizing the benefits of plug-in electric vehicles contracts with a comprehensive model of information-gap decision theory, J Energy Storage 32 (2020). https://doi.org/10.1016/j.est.2020.102010.

[40] X. Cao, J. Wang, J. Wang, B. Zeng, A Risk-Averse Conic Model for Networked Microgrids Planning with Reconfiguration and Reorganizations, IEEE Trans Smart Grid 11 (2020) 696–709. https://doi.org/10.1109/TSG.2019.2927833.

[41] M. Tostado-Véliz, H.M. Hasanien, A.R. Jordehi, R.A. Turky, F. Jurado, Risk-averse optimal participation of a DR-intensive microgrid in competitive clusters considering response fatigue, Appl Energy 339 (2023). https://doi.org/10.1016/j.apenergy.2023.120960.

[42] S. Nojavan, M. Majidi, K. Zare, Risk-based optimal performance of a PV/fuel cell/battery/grid hybrid energy system using information gap decision theory in the presence of demand response program, Int J Hydrogen Energy 42 (2017) 11857–11867. https://doi.org/10.1016/J.IJHYDENE.2017.02.147.

[43] M.A. Jirdehi, S. Ahmadi, The optimal energy management in multiple grids: Impact of interconnections between microgrid–nanogrid on the proposed planning by considering the uncertainty of clean energies, ISA Trans 131 (2022) 323–338. https://doi.org/10.1016/j.isatra.2022.04.039.